Hindawi
Shock and Vibration
Volume 2022, Article ID 1440477, 13 pages
https://doi.org/10.1155/2022/1440477

Research Article

Dynamic Response Analysis of Pile Group Foundation of Super-Giant Sewage Treatment Structure on Hydraulic Fill Foundation

Yi Huang,[1,2] **Xugang Chen**,[1] **Lijuan Cheng**,[1,2] **Tiyong Bai**,[1] **and Ru Yan**[1,2]

[1]*Chengdu Engineering Corporation Limited, Chengdu 611100, China*
[2]*Sichuan Urban Underground Space Survey Design and Construction Technology Engineering Laboratory, Chengdu 611100, China*

Correspondence should be addressed to Yi Huang; p2020233@chidi.com.cn

Received 25 April 2022; Revised 26 May 2022; Accepted 31 May 2022; Published 15 June 2022

Academic Editor: Yonggang Zhang

Copyright © 2022 Yi Huang et al. This is an open access article distributed under the Creative Commons Attribution License, which permits unrestricted use, distribution, and reproduction in any medium, provided the original work is properly cited.

In this study, a 3D numerical model, considering the dynamic interaction between soil, pile foundation, and super structure, and the parameter analysis of internal force response of pile group foundation under differences seismic intensity, was established based on the Bangladesh sewage treatment plant project to investigate the dynamic response of pile group foundation of liquid-containing structures. The results show that the internal force of pile gradually increases with time, and the horizontal dynamic displacement peak value appears earlier under different seismic wave responses and seismic intensity. With the increase of seismic time history, the variation degree of dynamic impedance with frequency and impedance peak will increase. The pile group effect and single pile bearing capacity of foundation in hydraulic fill fine sand and silty clay were verified. By comparing numerical simulation and theoretical calculation, the results show that the pile group foundation exerts the soil squeezing effect after pile construction is completed, and the dynamic elastic modulus of the soil layer can be increased. Simultaneously, the soil layer will have a better integral stiffness. The pile group effect coefficient obtained by the solid perimeter method is most consistent with the numerical simulation method.

1. Introduction

In recent years, international super-giant sewage treatment plant projects have been developed quickly in developing countries in Southeast Asia, where the stratum distribution is mostly dominated by silty clay and high liquid limit clay. On the other hand, pile foundation has been widely used by various structures for the characteristics of good stability, large bearing capacity, and small differential settlement, especially for seismic loading. It can be better adapted to complex geological conditions, which can transfer the load to the soil layer with good bearing performance in the deep underground [1, 2].

Under the action of the earthquake, the pile foundation is often affected by the stratum acceleration, which would result in the deformation and even damage of the main structure and pile top [3]. Exploring the dynamic interaction between pile foundation and soil is an urgent problem to be solved at present [4]. Besides, theoretical test and numerical simulation are the main methods to study the pile-soil interaction. Meanwhile, many scholars have investigated these issues through model tests [4], while researches on seismic response of pile foundation with high cushion cap mainly focus on laboratory quasi-static tests and shaking table or centrifuge model dynamic tests [5]. Wang et al. carried out a cyclic lateral loading test to study the seismic failure mechanism and ductile energy dissipation capacity of elevated RC pile-cap foundations, and the results have shown that plastic hinges were detected first at the top of the outer piles. [6]. Liu et al. [7] conducted a shake-table test on a 2×2 pile group to investigate the behavior of the pile group under the liquefaction-induced lateral spreading and the liquefied

soil pressure; meanwhile, the numerical simulation was implemented, and the results showed that permanent pile head displacement is about 31 mm that is far less than the ground surface displacement of 120 mm. Qin and Ma [8] investigated the seismic behaviors of piles under high-raft conditions by centrifuge tests and the finite element method, and the results indicated that the main seismic failure mechanism is the liquefaction of lateral expansion foundation for a pile foundation in sandy soil.

In fact, compared with theoretical analysis and numerical calculation, physical tests are more realistic. However, it has high requirements for device configuration. In this case, due to the influence of site and cost, many full-scale tests cannot be carried out, and this results in inconsistency with the reality [9]. On the other hand, the finite element method (FEM) has been widely developed because of the merits of good repeatability, high efficiency, and parameter analysis [10]. It can consider the linear and nonlinear characteristics of soil and pile and can well simulate the seismic action of the soil. Zhuang et al. analyzed the three-dimensional liquefaction large deformation by using numerical simulation and verified the reliability of the model in the ABAQUS development subroutine [11]. In addition, many scholars compared experiment test with numerical simulation to verify the authenticity of the experiment test [12]. Therefore, numerical simulation has become an important means to investigate the interaction between pile-soil and the main structure [13, 14]. Unfortunately, under the current international engineering background, researches on the structural foundation treatment method of international large-scale sewage treatment plant are rarely carried out [15–17], and more works more work should be carried out.

In this study, based on the largest sewage treatment plant in South Asia, the nonlinear dynamic time-history response analysis method is used to comprehensively study the dynamic characteristics and pile-soil interaction mechanism in sewage treatment plant structure [18]. Using MIDAS/GTS NX, a 3D numerical calculation model, focused on the internal force and displacement change of nonlinear time history dynamic response of pile groups under different seismic waves, was established, and peak internal force and relative displacement of pile foundation under different earthquakes were analyzed comprehensively. The numerical simulation results provide theoretical research and technical support for the design scheme.

2. Project Background

The project is located in the east of Gojaria River, Dasharkandi District, Dhaka City, and the Dasherkandi sewage treatment plant mainly disposes sewage water from Dasherkandi, Hatirjheel, Gulshan, Banani, and other areas to eliminate the current sewage pollution to Balu River. The project location is shown in Figure 1. The scope of works for the Dasherkandi sewage treatment plant in Bangladesh includes a sewage pump lifting station, sewage conveyance pipeline (2×4.8 km), and secondary sedimentation tank (hereafter in SST).

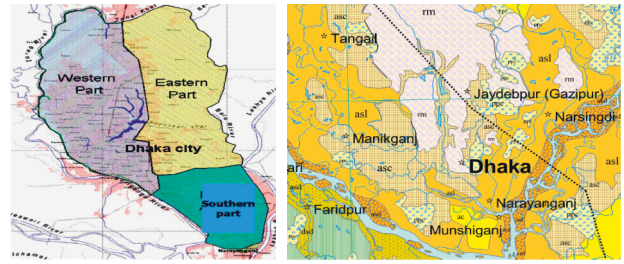

Figure 1: Project site location maps.

The secondary sedimentation tank is a reinforced concrete water storage structure with a top elevation of RL+11.77 m, the bottom elevation of RL+6.180 m, the outside elevation of RL + 8.500 m, and the diameter of the SST is 55.0 meters. More details information and the 3-D numerical calculation model are shown in Figures 2–4, respectively.

3. Numerical Model and Calculation Parameters

3.1. Numerical Model. Considering the situation of the project and the boundary effect, the upper boundary is free, and the vertical surrounding surface is constrained by a free field, while the lower surface is fixed constraint. The geometric dimensions of the model are 120 m in length and width, and the total height of the stratum is 45.6 m (Figure 3). The model includes 46192 3D soil units, 3696 2D sewage structure plate units, and 3234 1D pile foundation units. Moreover, the Mohr-Coulomb model is adopted for soil mass, while the sewage structure and pile foundation are established by the concrete unit which considered the elastic deformation. The calculation conditions are mainly divided into three parts: the original ground settlement (completed), the completion of the construction period, and the input of seismic acceleration.

In the calculation of the original ground settlement, as soon as the construction period was completed, pile foundation and structure units were activated. During the earthquake period, the stress conditions mainly include the ground acceleration, while the soil around the structure is usually a semi-infinite medium. When analysing the dynamic interaction between soil and structure, the finite soil cannot be simply intercepted for the dynamic analysis of soil structure. As a result, it made lateral soil adopts a viscoelastic boundary to absorb seismic wave energy.

3.2. Calculation Parameters. The soil layer from top to bottom is high liquid limit clay, medium-high liquid limit clay, fine sand (medium dense), and medium-high liquid limit clay fine sand (medium dense-dense) layer, respectively. The cast-in-place concrete piles were distributed at the bottom slab of the structure. The tank walls, bottom slabs, and piles are simulated by plate element and beam element, respectively. Considering that the pile foundation may rotate

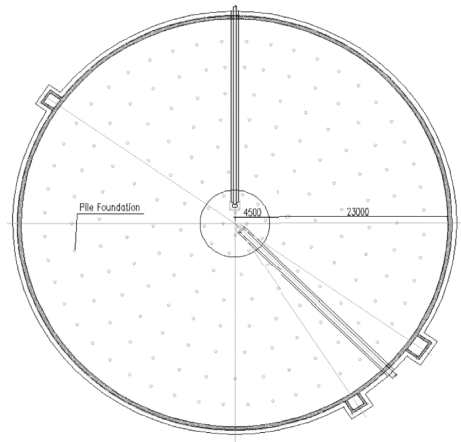

Figure 2: Typical layout for SST.

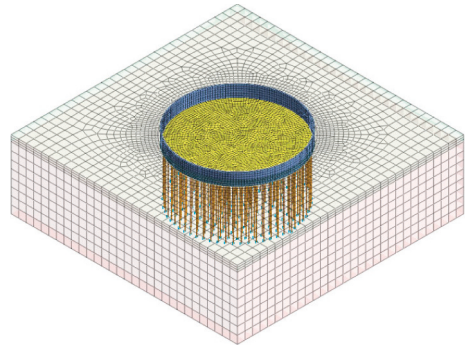

Figure 3: Numerical calculation 3-D model for SST.

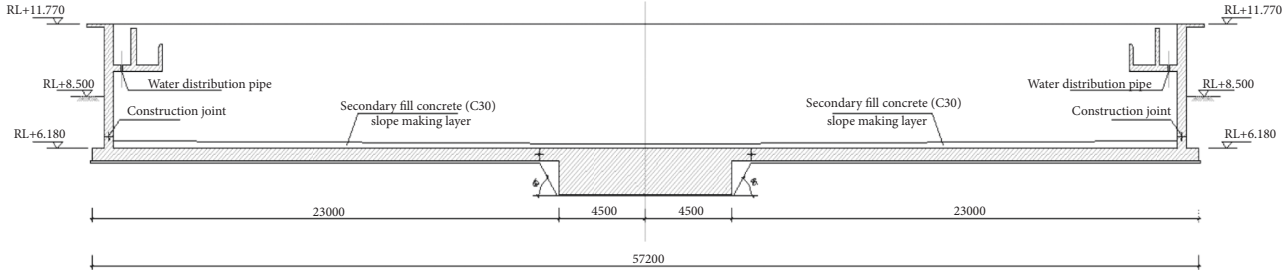

Figure 4: Typical section for SST (unit: m).

greatly under the action of the earthquake, the Ry rotation constraint is released at the joint between the pile top and the bottom slab of the structure. The soil layer parameters are tabulated in Table 1.

3.3. Seismic Waves Parameters. During the dynamic time history analysis, factors such as peak acceleration, spectrum characteristics, and duration of vibration should be considered to select the seismic wave [19]. According to the site category of the project, four types of seismic waves are selected. The seismic wave is input from the bedrock [20], the time interval is 0.01 s, the total calculation time is 30 s, and the peak acceleration is 0.15–0.25 g. The time history curves of seismic waves are shown in Figures 5–8.

In order to fully obtain the relative deformation effect of the structure, it is assumed that the site is composed of multiple horizontal infinite strata, the vibration is caused by shear wave, the vibration is only horizontal vibration, and the shear wave can be transmitted and reflected vertically between the strata [21]. Therefore, the lateral boundary of the model foundation adopts the free field boundary. Moreover, it is assumed that the sandy soil layer is the undrained boundary, and the other soil layers are the free vertical drainage boundary.

3.4. Nonlinear Dynamic Time History Analysis Theory. The nonlinear analysis includes geometric nonlinear and material nonlinear calculations [22]. The whole analysis is based on implicit integration theory. The dynamic balance

Table 1: Value of formation physical and mechanical parameters.

Layer	Soil name	Thickness of layer (m)	Calculation parameters		
			Density ρ (g/cm^3)	Cohesion c (kPa)	Friction angle Φ (°)
1	High liquid limit clay	2.80	18.65	1.90	17.25
2	Medium-high liquid limit clay	2.50	19.86	9.50	25.08
3	Fine sand (medium dense)	4.60	20.25	2.12	19.62
4	Medium-high liquid limit clay	4.85	20.55	9.84	26.85
5	Fine sand (medium dense)	10.80	21.84	1.22	20.87
6	Fine sand (very dense)	14.70	22.45	13.40	18.32

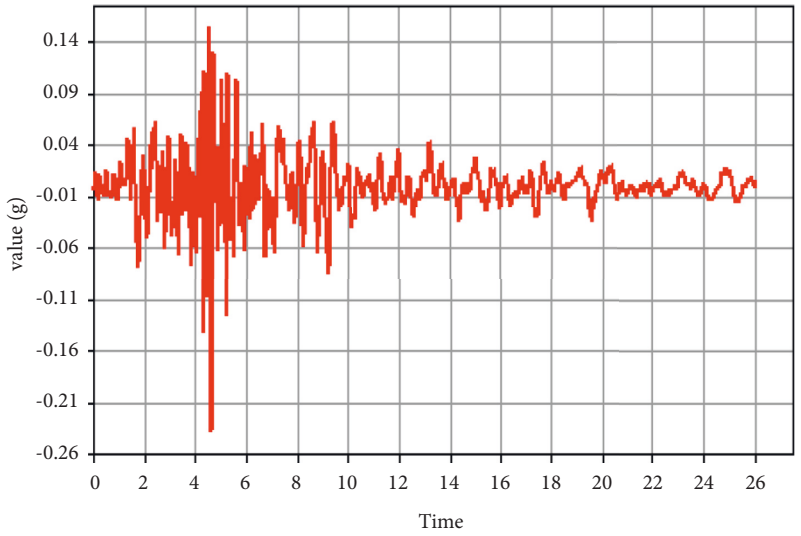

Figure 5: Seismic wave I (0.1524 g).

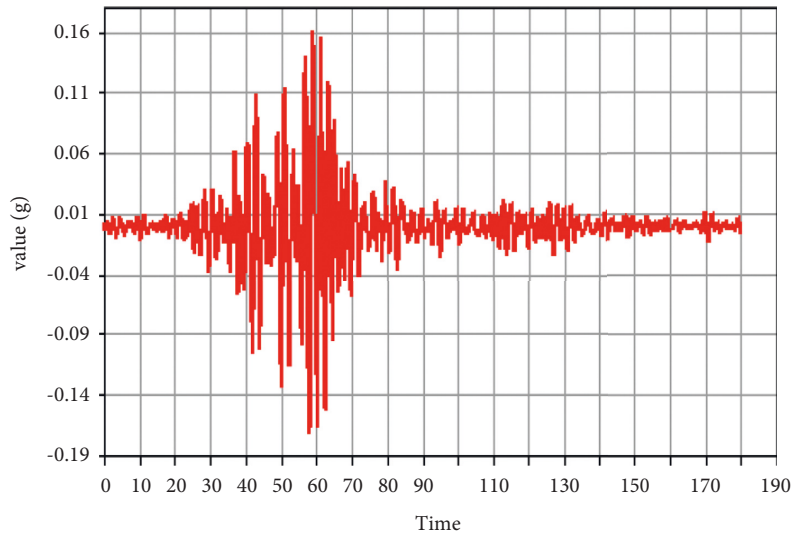

Figure 6: Seismic wave II (0.1714 g).

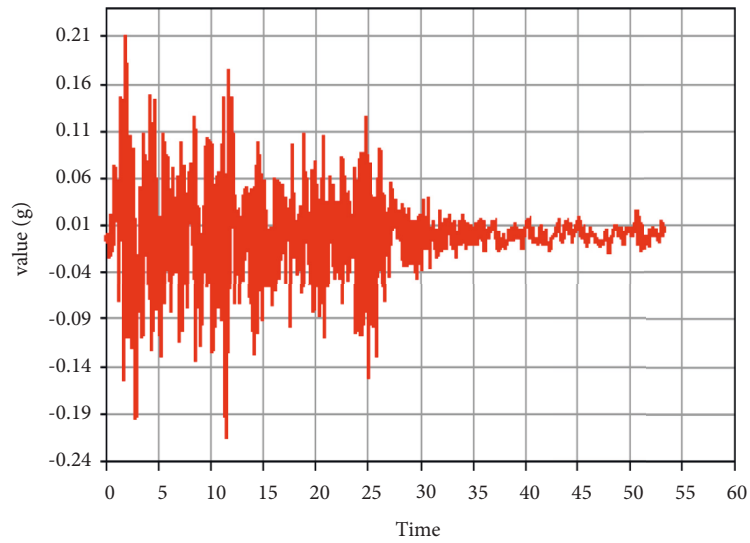

Figure 7: Seismic wave III (0.2114 g).

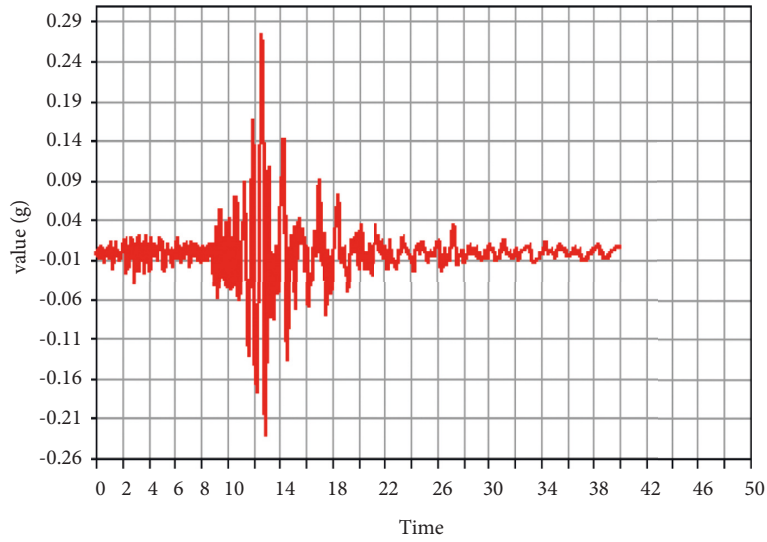

Figure 8: Seismic wave IV (0.2504 g).

equation of nonlinear time history analysis is implicitly time-integrated by the HHT-a method. The specific expression is as follows [21]:

$$\left(\mathrm{Ma}^{n+1}\right) + (1 + a_H)\left[Cv^{n+1} + f^{\mathrm{int},n+1} - f^{\mathrm{ext},n+1}\right] - a_H\left[Cv^{n} + f^{\mathrm{int},n} - f^{\mathrm{ext},n}\right] = 0, \quad (1)$$

where M is the mass matrix, a^{n+1} and v^{n+1} are the acceleration and speed of $n+1$ time step. a_H is the damping effect coefficient; meanwhile, $f^{\mathrm{int},n}$ and $f^{\mathrm{ext},n}$ are the internal force and external force obtained through element displacement, velocity, and acceleration in the n-th time step, respectively.

In the nonlinear analysis, the influence of the rotational mass matrix caused by geometric nonlinearity is considered. Therefore, the moment of inertia of the mass matrix must be corrected in each iterative calculation according to the limited rotation of the reference node. In addition, the inertial force generated by the change rate of the mass stiffness matrix also needs to be considered [23]. C is the damping effect in the time history analysis, which considers the stiffness matrix and mass matrix at the boundary of the model, and is presented by the following matrix.

$$C = a_j^e M_j^e + \beta_j^e K_j^e + B, \quad (2)$$

where a_j^e is the mass proportional damping coefficient of the j-th element, the M_j^e is the mass matrix of unit j. Meanwhile, the a_j^e is the stiffness proportional damping coefficient of the j-th element, the K_j^e is the stiffness matrix of the j-th element, and the B is the damping matrix of the damping element.

As per the time step equation of the Newmark method [24], the expressions of velocity, displacement, and acceleration in the n-th and $n+1$ time step are as follows:

$$v^{n+1} = v^n + \Delta t\left[\gamma a^{n+1} + (1-\gamma)a^n,\right.$$
$$u^{n+1} = u^n + \Delta t v^n + \frac{1}{2}\Delta t^2\left[2\beta a^{n+1} + (1-2\beta)a^n,\right. \quad (3)$$

where $\gamma = (1-2a_H)/2$ and $\beta = (1-2a_H)^2/4$, $a_H = -0.05$ is the default value, which is consistent with the linear time history analysis method.

4. Analysis of Calculation Results

4.1. Pile Foundation Internal Force. It can be seen from Figures 9 and 10 that under the action of different types of seismic waves, the change law of the time-history response of the pile top acceleration is different; meanwhile, the amplitude, acceleration peak value, and the time of occurrence are significantly different [25].

Since the ground motion load is a cyclic load, positive and negative values in the time history curve only represent the seismic direction. For the analysis of the internal force for the pile foundation, the peak value plays a dominant role, so the absolute value is used to analyze the variation law of the acceleration peak value. Figures 11–16 extract the absolute maximum values of internal force and displacement of pile group foundation.

4.2. Relative Displacement of Pile Top. Since the top of the pile is fixed with upper structure, the boundary conditions are assumed to be 0 for the rotation angle and displacement at the pile end, the relative displacement X of the pile body displacement is calculated, and the time history response of the pile foundation at different depths is obtained by extracting the time history. The pile-soil relative displacement is obtained by the difference between the displacement of the pile and the displacement of the soil [26].

By analysing the distribution of bending moment, the internal force of a typical pile foundation, and the results of relative displacement of pile foundation, we found that the maximum horizontal deformation displacement of the pile foundation is the connection with the bottom slab at the outer edge of the structure, and the bending moment stress here is also the largest, while the structure set on the upper part of the foundation is subjected to uniformly distributed load, and the vertical support stiffness distribution of foundation or pile group changes in location distribution due to the interaction between soil and pile foundation. Figure 17 shows that the settlement deformation appears as a dished distribution with large inside and small outside, while the base reaction appears as a saddle distribution with small inside and large outside. According to the load distribution law, the piles should be relatively concentrated in the center of the structure, and the external area should be appropriately weakened. While the length should be reduced for the outer piles.

Figure 18 shows the relative displacement curve of pile top under seismic period, while Figure 19 shows the spectrum curves of pile foundation moment response after FFT transformation under different seismic waves. It can be seen that with the action of the earthquake, multiple peaks appear in the spectrum of pile internal force in the range of 0.2–8.0 Hz, and the frequency corresponding to the maximum amplitude is near 0.3 Hz.

After the pile foundation construction is completed, the overall stiffness of the foundation increased to a certain extent, while the pile foundation compaction foundation is formed successfully, which improves the structural safety and foundation stability under seismic conditions. The peak frequency of the internal force of the pile body is mainly distributed in the range of 0.2–5.0 Hz, which is smaller than that before the pile foundation construction. Within a certain range, the resonance frequency range generated by the seismic wave can be avoided, which is more favorable for the internal force response under the action of the seismic wave.

5. Study on Effect Coefficient of Pile Groups

Under the vertical load, the interaction between the pile group foundation and the surrounding soil causes the superposition of the foundation stress, which makes the stress mechanism of pile-soil more complicated [27]. The deformation and failure characteristics of the pile group are obviously different from those of single piles, and the bearing capacity of the pile group is not equal to the result of the addition of the bearing capacities of all single foundation piles [28]. This phenomenon is so-called the "pile group effect." The strength of the pile group effect is generally measured by the pile group effect coefficient, which is defined as

$$\eta = \frac{W_u}{n \times P_u}, \quad (4)$$

where P_u is the ultimate bearing capacity of a single pile. W_u is the ultimate bearing capacity of the pile group; n is the number of piles (the number of foundation piles in the pile group). In this project, the main characteristics of the pile group effect are the vertical bearing capacity.

At this stage, there are mainly the following five calculation methods for determining the pile group effect coefficient. Seiler Keeney method is suitable for high pile-cap foundation [29], and the factors considered are relatively single. The partial coefficient rule is based on a large number of field true tests for research and analysis, which requires a large amount of resources. The stress superposition law comprehensively considers the influence of pile spacing, pile number, pile length, soil characteristics, and other factors [30] and has a certain degree of rationality, which is in line with the actual situation of the pile group pile foundation studied in this paper. Although the calculation formulas given by the solid perimeter method only consider the influence of pile distance, it can still be compared with the calculation results of the numerical simulation method in this paper. Therefore, the established pile group foundation is used for comparative analysis in this section.

When analysing the relationship between pile group effect coefficient and pile spacing, the vertical bearing

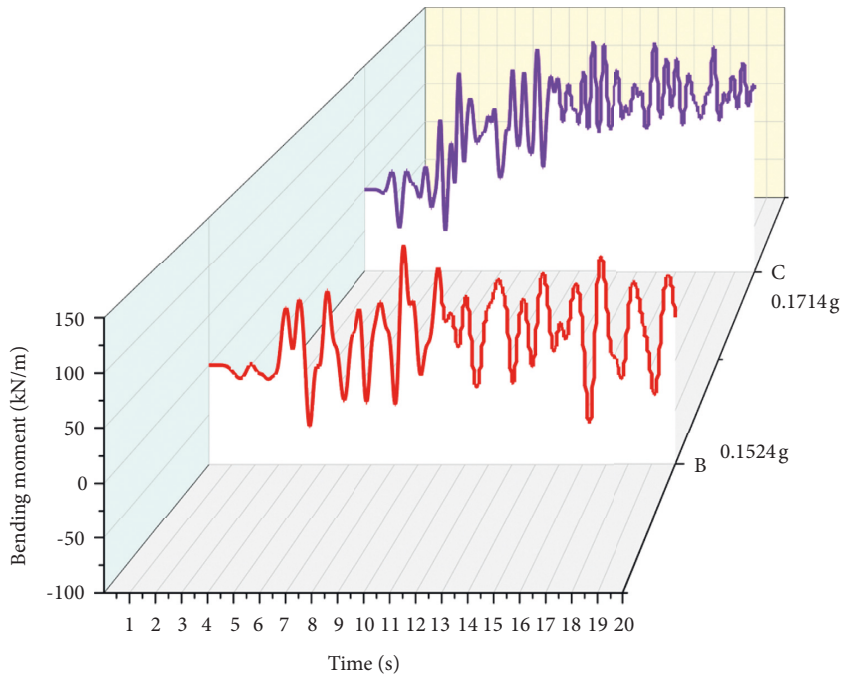

Figure 9: Top of pile bending moment for time-history curve-a.

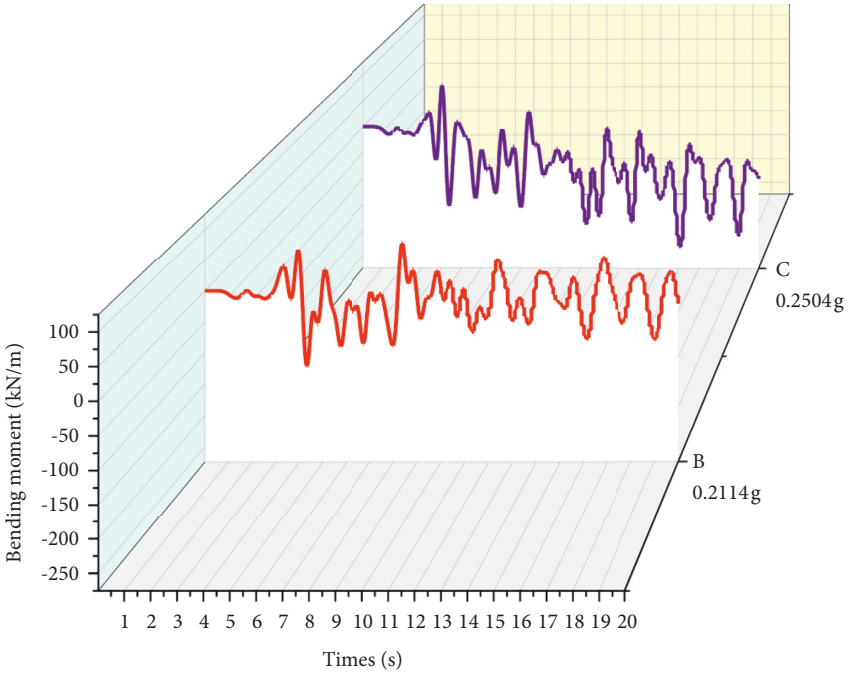

Figure 10: Top of pile bending moment for time-history curve-b.

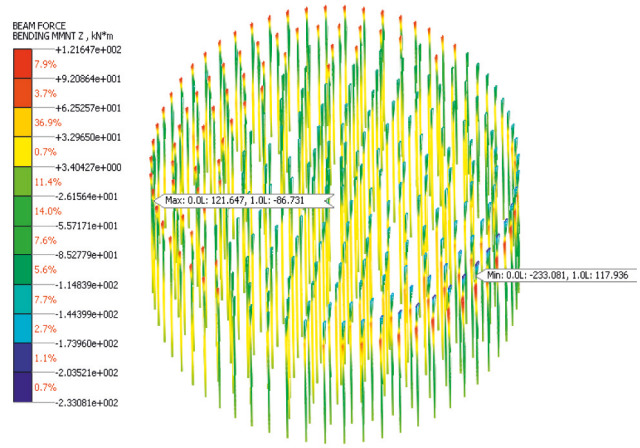

Figure 11: Bending moment distribution diagram of pile group (maximum moment).

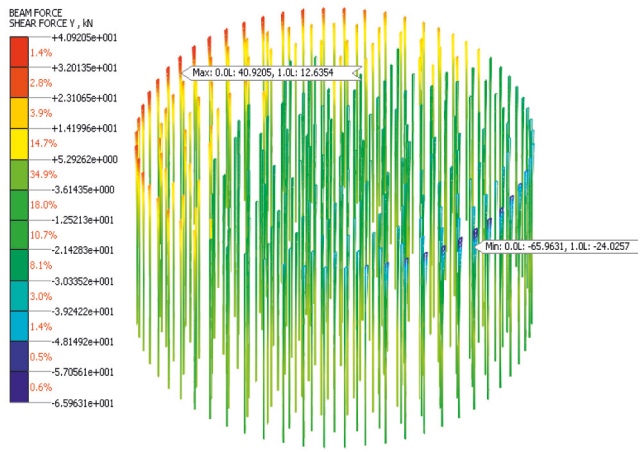

Figure 12: Shear force distribution diagram of pile group (maximum moment).

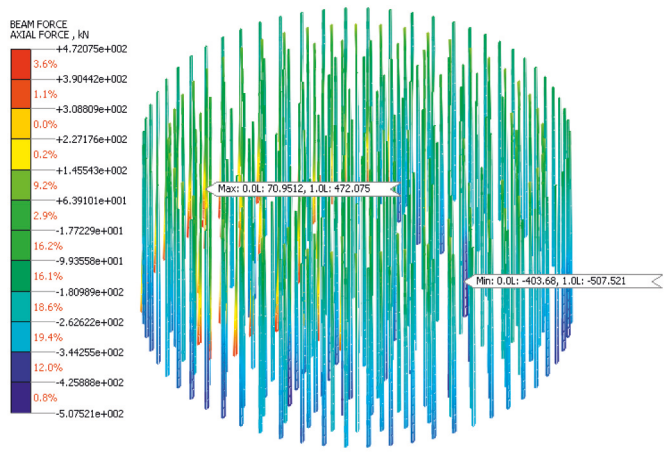

Figure 13: Axial force distribution diagram of pile group (maximum moment) (absolute MAX).

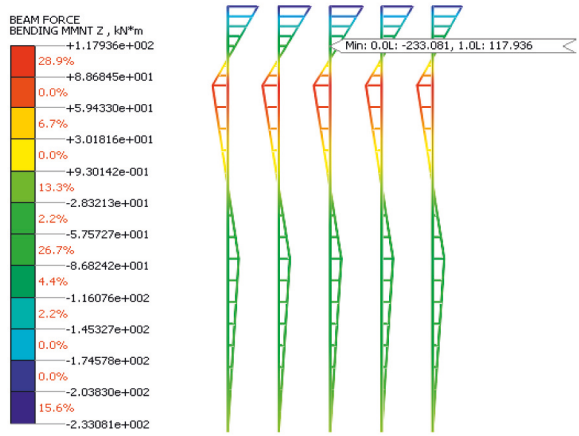

Figure 14: Cloud diagram of bending moment distribution of typical pile foundation.

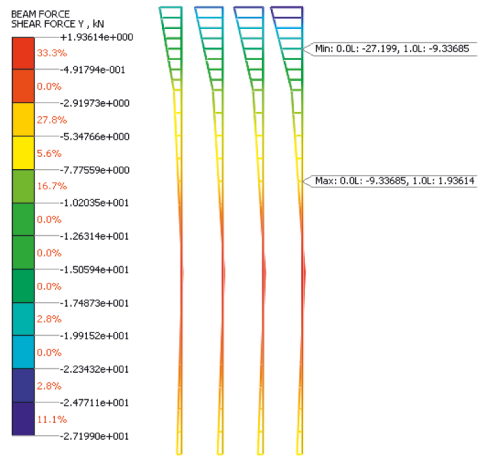

Figure 15: Cloud diagram of shear force distribution of typical pile foundation.

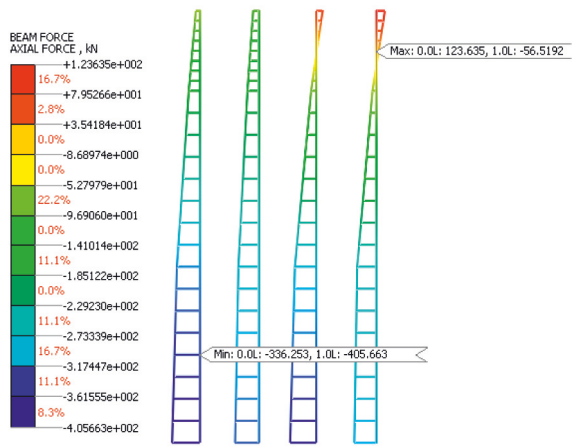

Figure 16: Cloud diagram of axial force distribution of typical pile foundation.

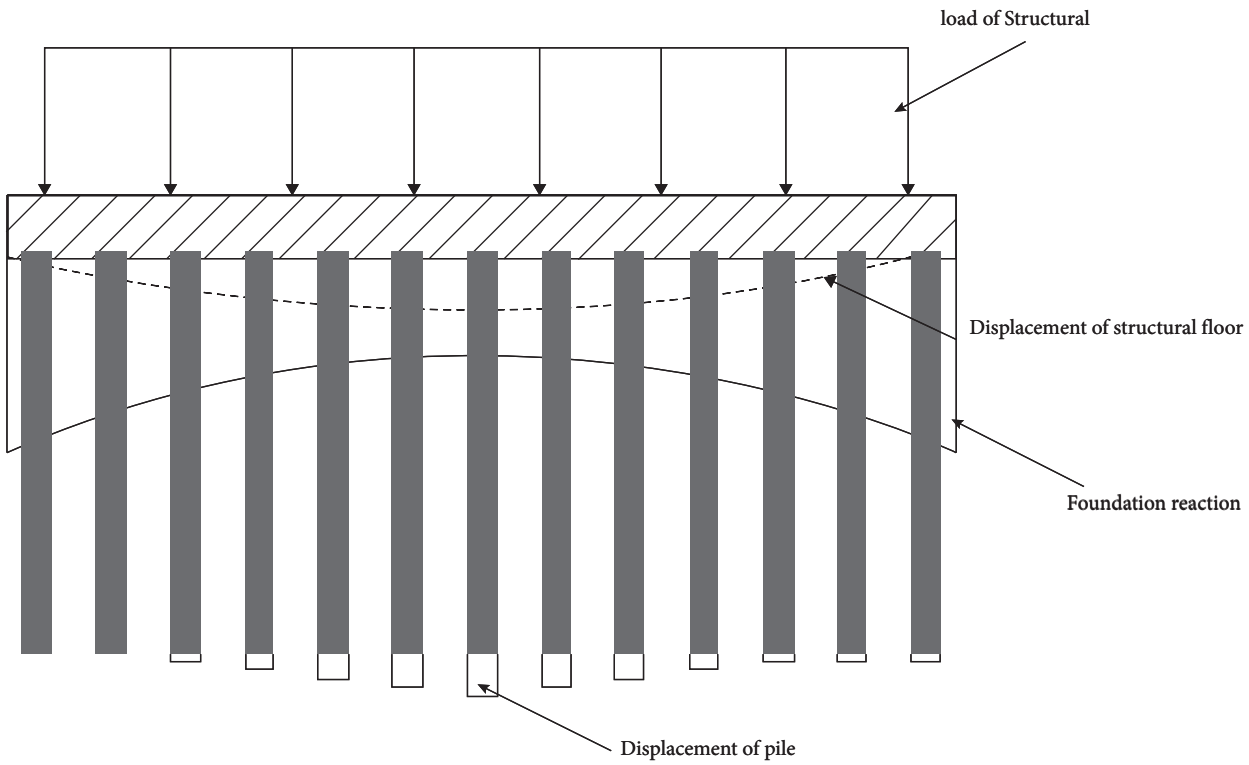

Figure 17: Schematic diagram of deformation characteristics of pile group stress system.

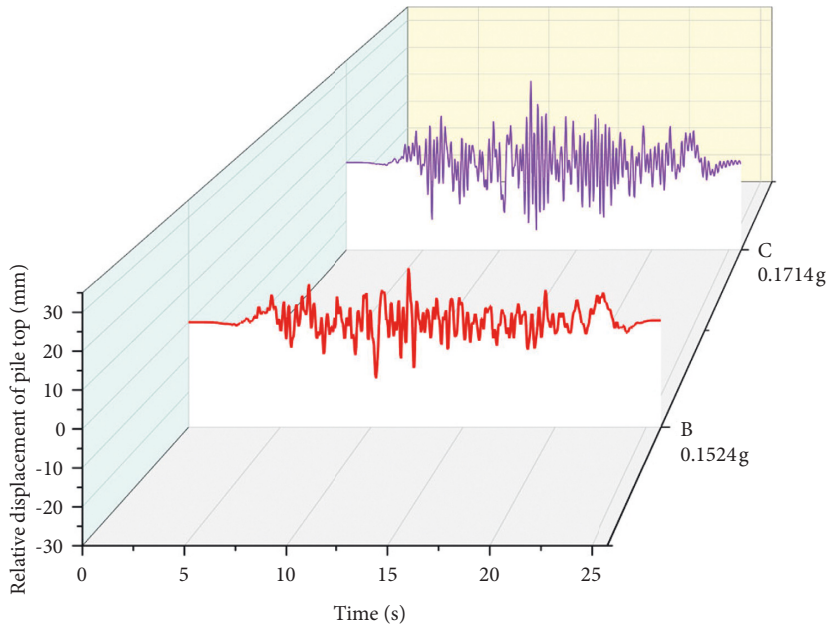

Figure 18: Relative displacement of pile top.

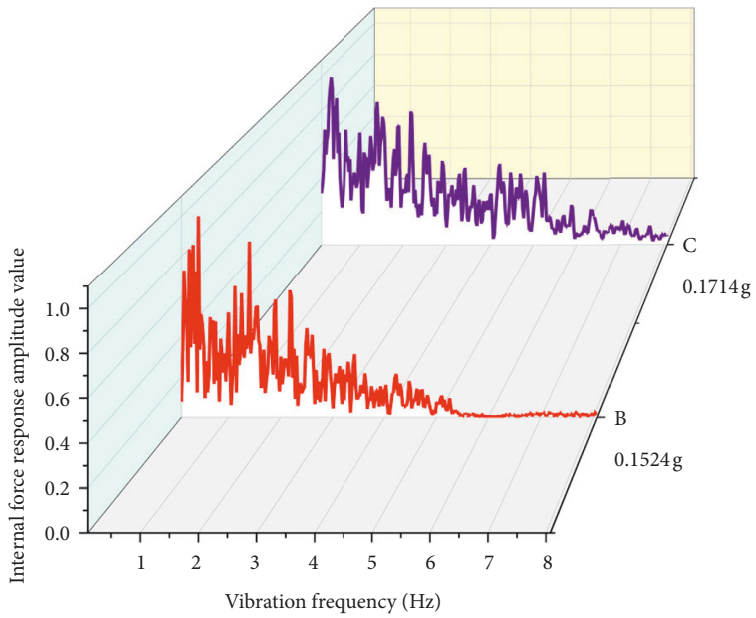

Figure 19: Vibration spectrum curve of pile foundation.

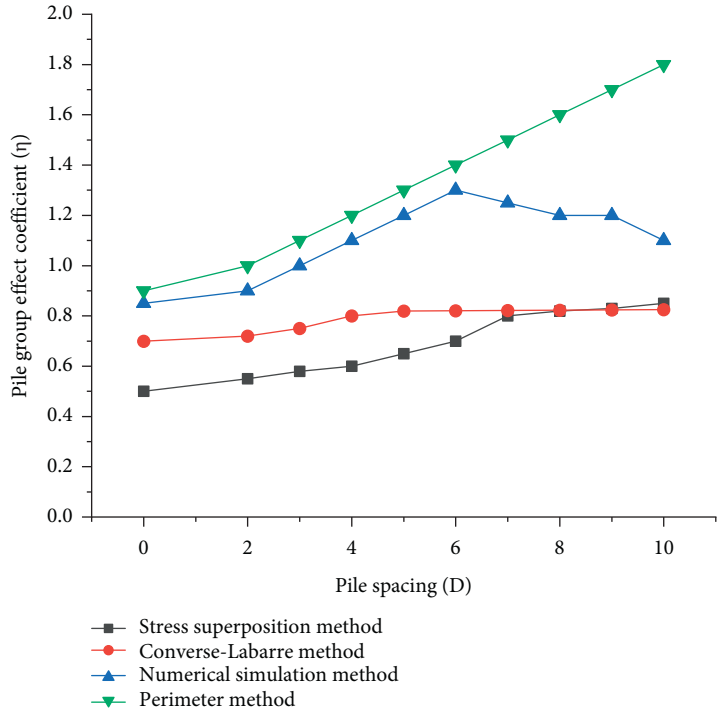

Figure 20: Comparison diagram of pile group effect coefficient.

capacity of the pile group takes the limit value of numerical simulation under different pile spacing. Figure 20 shows the relationship curve of pile group effect coefficient of numerical simulation method under compressive load with pile spacing and compared with various methods. It can be seen that the pile group is calculated by each method.

6. Conclusion

In order to study the reliability of pile group foundation for large structures, in the present study, the engineering site of Bangladesh silty clay is selected for pile group dynamic nonlinear time history analysis, and the numerical simulation analysis is carried out. The main conclusions are as follows.

(1) Under different seismic conditions, the load bending moment curve of the pile group belongs to slow variation, and the axial force of the pile body increases with the load. As a result, while the natural foundation meets the requirement of bearing capacity, the edge area of the structure with high load concentration and the middle area of the structure with large settlement should be strengthened partly. Simultaneously, based on the design requirements of the code, it is particularly critical to carry out the joint analysis and calculation of the overall soil, pile foundation, and structure, which can further optimize the pile foundation arrangement.

(2) The displacement curve of time obtained is basically consistent with the field measured curve, and the results of numerical simulation are reliable. The response displacement method can be used for comparison and calculation in future research. The change of the pile group effect coefficient is studied by changing the pile spacing. It is suggested that the pile spacing in the preliminary design should be 4D~5D.

(3) The strain response amplitude of the corner pile is significantly greater than that of the middle pile foundation, meaning that the corner pile is more prone to seismic damage at the top of the pile. Before foundation liquefaction, the maximum bending moment amplitude of the pile group foundation appears in the middle and upper part of the pile body at the corner, but the bending moment amplitude of the pile top increases sharply after foundation liquefaction. Compared with the model test and numerical calculation results of existing soil-pile structure dynamic interaction, the rotation effect of the foundation of seismic isolation structure increases sharply after foundation liquefaction. The main reason is related to the dynamic interaction of soil pile isolation layer upper structure; meanwhile, the findings above need to be further verified by numerical simulation and theoretical analysis.

Data Availability

The data used to support the findings of this study are included in the article.

Conflicts of Interest

The authors declare that they have no conflicts of interest in this study.

Acknowledgments

This paper was supported by the Research Project Fund of China Power Construction Group Chengdu Survey, Design and Research Institute, and Research Project Fund of Key Technologies for the Development and Utilization of Large Urban Underground Space (p34616).

References

[1] B. B. Sheil, B. A. Mccabe, E. M. Comodromos, and B. M. Lehane, "Pile groups under axial loading: an appraisal of simplified non-linear prediction models," *Géotechnique*, vol. 69, no. 7, pp. 565–579, 2019.

[2] S. B. Magade and R. K. Ingle, "Analysis methods for pile foundation: a critical review of the literature and recommended suggestions," *Innovative Infrastructure Solutions*, vol. 6, no. 1, p. 14, 2020.

[3] H. Nagai, "Simplified method of estimating the dynamic impedance of a piled raft foundation subjected to inertial loading due to an earthquake," *Computers and Geotechnics*, vol. 105, pp. 69–78, 2019.

[4] Y. Li, J. Zhang, H. Chen, and D. Y. Qiang, "Study on the dynamic response characteristics and p-y curve of straight and inclined pile groups in saturated sands," *Applied Sciences*, vol. 12, no. 5, p. 2363, 2022.

[5] C. Zhang, Z. Feng, Y. Guan, and H. F. B. Chen, "Study on liquefaction resistance of pile group by shaking table test," *Advances in Civil Engineering*, vol. 2022, pp. 1–12, Article ID 5074513, 2022.

[6] X. Wang, A. Ye, Z. He, and Y. Shang, "Quasi-static cyclic testing of elevated rc pile-cap foundation for bridge structures," *Journal of Bridge Engineering*, vol. 21, no. 2, Article ID 04015042, 2016.

[7] C. Liu, L. Tang, X. Ling, and L. L. X. Deng, "Investigation of liquefaction-induced lateral load on pile group behind quay wall," *Soil Dynamics and Earthquake Engineering*, vol. 102, pp. 56–64, 2017.

[8] H. Qin and K. Ma, "Dynamic behaviour difference between high- and low-raft forms of piles in earthquakes," *Geotechnical Research*, vol. 8, no. 3, pp. 85–92, 2021.

[9] Y. Yin, Q. Li, and L. Qiao, "Response of energy pile-soil structure and pile group effect: an indoor similarity simulation study," *Journal of Building Engineering*, vol. 51, Article ID 104247, 2022.

[10] M.-h. Zhao, S. Heng, and Y. Zheng, "Numerical simulation on behavior of pile foundations under cyclic axial loads," *Journal of Central South University*, vol. 24, no. 12, pp. 2906–2913, 2018.

[11] H. Zhuang, Z. Hu, X. Wang, and G. Chen, "Seismic responses of a large underground structure in liquefied soils by fem numerical modelling," *Bulletin of Earthquake Engineering*, vol. 13, no. 12, pp. 3645–3668, 2015.

[12] Q. Liu, H. Zhuang, Q. Wu, K. Zhao, and G. Chen, "Experimental study on dynamic modulus and damping ratio of rubber-sand mixtures over a wide strain range," *Journal of Earthquake and Tsunami*, vol. 16, no. 02, 2022.

[13] K. Jones, M. Sun, and C. Lin, "Numerical analysis of group effects of a large pile group under lateral loading," *Computers and Geotechnics*, vol. 144, Article ID 104660, 2022.

[14] D. Kong, M. Deng, and Y. Li, "Numerical simulation of seismic soil-pile interaction in liquefying ground," *IEEE Access*, vol. 8, pp. 195–204, 2020.

[15] Q. Wu, X. Ding, Y. Zhang, and Z. Y. Chen, "Numerical simulations on seismic response of soil-pile-superstructure in coral sand," *Ocean Engineering*, vol. 239, Article ID 109808, 2021.

[16] A. Majeed and O. Haider, "Simulation of bearing capacity of bored piles," *MATEC Web of Conferences*, vol. 162, p. 01004, 2018.

[17] R. Chmielewski, L. Kruszka, and P. Muzolf, "The selection of methods for strengthening of the reinforced-concrete structure of the open tank," *Case Studies in Construction Materials*, vol. 12, Article ID e00343, 2020.

[18] Y. X. He, Y. Qiang, and L. Li, "Research on the dynamic response of dam under rare earthquake through dynamic time-history analysis method," *Advanced Materials Research*, vol. 594, pp. 1640–1644, 2012.

[19] G. M. Álamo, J. D. R. Bordón, and J. J. Aznárez, "On the application of the beam model for linear dynamic analysis of pile and suction caisson foundations for offshore wind turbines," *Computers and Geotechnics*, vol. 134, Article ID 104107, 2021.

[20] I. K. Fontara, P. S. Dineva, G. D. Manolis, and F. Wuttke, "Numerical simulation of seismic wave field in graded geological media containing multiple cavities," *Geophysical Journal International*, vol. 206, no. 2, pp. 921–940, 2016.

[21] H. C. Bernardes, S. L. Carvalho, and M. M. Sales, "Hybrid numerical tool for nonlinear analysis of piled rafts," *Soils and Foundations*, vol. 59, no. 6, pp. 1659–1674, 2019.

[22] F. González, L. A. Padrón, J. J. Aznárez, and O. Maeso, "Equivalent linear model for the lateral dynamic analysis of pile foundations considering pile-soil interface degradation," *Engineering Analysis with Boundary Elements*, vol. 119, pp. 59–73, 2020.

[23] J. M. Dickens, J. M. Nakagawa, and M. J. Wittbrodt, "A critique of mode acceleration and modal truncation augmentation methods for modal response analysis," *Computers & Structures*, vol. 62, no. 6, pp. 985–998, 1997.

[24] C. Shuenn-Yih, "Studies of Newmark method for solving nonlinear systems. Part I. Basic analysis," *Journal of the Chinese Institute of Engineers*, vol. 27, no. 5, pp. pp651–62, 2004.

[25] H. Jiang, Z. Wang, X. Bai, C. Zeng, and M. Wang, "Nonlinear responses and damage characteristics for group-piles foundation of a deep-water bridge under strong near-fault and far-field earthquakes," *Journal of Vibration and Shock*, vol. 36, no. 24, pp. 13–22, 2017.

[26] A. M. Kaynia, "Dynamic response of pile foundations with flexible slabs," *Earthquakes and Structures*, vol. 3, no. 3_4, pp. 495–506, 2012.

[27] B. Tang and X. Chen, "Finite element analysis of effect of pile group," *Rock and Soil Mechanics*, vol. 26, no. 2, pp. 299–302, 2005.

[28] Z. Kang, B. Wu, and S. Zhang, "Analysis and calculation of bearing capacity of pile groups in sandy soil," *Journal of PLA University of Science and Technology (Natural Science Edition)*, vol. 17, no. 2, pp. 121–125, 2016.

[29] Z. Xiongwen, X. Dong, and L. I. Zhen, "Pile group effect of main pylon foundation of sutong bridge," *Journal of Hohai University. Natural Sciences*, vol. 34, no. 2, pp. 200–203, 2006.

[30] N. Djarwanti, R. Harya Dananjaya, and F. Prasetyaningrum, "Development of graphical method of pile group foundation design," *Applied Mechanics and Materials*, vol. 845, pp. 94–99, 2016.

[31] Z. Li, S. Escoffier, and P. Kotronis, "Centrifuge modeling of batter pile foundations under sinusoidal dynamic excitation," *Bulletin of Earthquake Engineering*, vol. 14, no. 3, pp. 673–697, 2015.